*Int. J. Mol. Sci.* **2007**, *8*, 259-272

International Journal of
**Molecular Sciences**
**ISSN 1422-0067**
© 2007 by MDPI
www.mdpi.org/ijms/

# The SPASIBA Force Field for Studying Iron-Tannins Interactions : Application to $Fe^{3+}/Fe^{2+}$ Catechol Complexes

**D. Yapo-Kicho, P. Lagant and G. Vergoten***

Glycobiologie Structurale et Fonctionnelle, UMR 8576 CNRS, Université des Sciences et Technologies de Lille, Bât. C9, 59655 Villeneuve D'Ascq France

*Author to whom correspondence should be adressed : gerard.vergoten@univ-lille1.fr

*Received: 23 January 2007 / Accepted: 2 March 2007 / Published: 30 March 2007*

---

**Abstract :** The SPASIBA force field parameters have been obtained for $Fe^{3+}/Fe^{2+}$-Oxygen interactions occuring between non-heminic iron and hydroxyl groups of polyphenols found in tannins. These parameters were derived from normal modes analyses based on quantum chemical calculations using the Density Functional Theory (DFT). Four models involving complexation of iron with water ($[Fe(H_2O)_6]^{3+}$, $[Fe(H_2O)_6]^{2+}$) and with cathechol molecules ($[Fe(cat)_2(H_2O)_2]^{-1}$, $[Fe(cat)_2(H_2O)_2]^{-2}$) were studied using the Density Functional Theory and the B3LYP hybrid functional under high spin states of iron.

**Keywords:** (FeIII/FeII)-Poyphenols interactions, Tannins, Density Functional Theory, SPASIBA force field.

---

## 1. Introduction

Iron and Tannins (polyphenolic compounds) present in vegetables are part of very important nutrient components for human organisms because of the participation of iron in a large variety of metabolisms and the benefical effects of tannins in the treatment of cardiovasular diseases[1-4].

Non heminic iron ($Fe^{3+}\backslash Fe^{2+}$) ions present in food display a weak intestinal absorption, worsened by a strong decrease in its availability originating from the appearance of very stable and irreversible complexes with hydroxyl groups present in tannins (polyphenols).

Ealier conformational analyses and complexation investigations on Tannins were first carried out using X-Rays crystallographic studies , NMR experiments using Molecular Mechanics to extract low energy-minimized structures reproducing coupling constants and NOE effects[5,6]. Molecular Modelling methods such as Docking-Scoring , 3D QSAR or Ligand Base Virtual Screening have

shown their utility to approach the conformational structure of Tannins in interactions with specific receptors [7]. These methods lead only to a static point of view describing the ability of polyphenols to interact with a large variety of biomolecules and inorganic ions. Empirical methods and, to a less extent, quantum chemical studies are able to give a dynamical point of view on the way that polyphenols can interact with their ligands , both considering their electronic properties and their intrinsic potential energy properties .

A comprehensive description of the geometrical and electronic properties implied in such complex appears as a first task to gain some knowledge about the mechanisms of complex formation. For this purpose, the Density Functional Theory (DFT) was used, in one hand, to identify various possible types of complexations and, in a second hand, to obtain the empirical SPASIBA force field parameters from vibrational spectra in order to perform further molecular dynamical studies.

## 2. Theoretical Calculations

### *2.1. Density Functional Theory*

DFT optimizations of the different complexes were performed using the B3LP hybrid density functional. Iron-water and iron-catechol complexes are well known to appear under a high spin state for iron [8-9] and different basis sets have been shown to be adequate when using hybrid functionals[10].

An extensive review on the structural and spectroscopic (UV absorption, NMR) characteristics of catecholato iron III complexes in catechol dioxygenases observed in various solvents or under tri or tetradentate ligands forms was reported by Yamahara et al. [9]. These last authors reported cis form for catechol rings bound to iron (III) as observed by X-rays studies on protocatechuate 3,4 dioxygenase (3,4-PCD). This form was found to be less stable than the trans form which was chosen in this study.

Iron III adopts a $3d^5$ electronic configuration and in the presence of a strong field environment displays a repartition of its d orbitals in two kinds of Molecular Orbitals i.e ; $e_g$ ($d_{z2}$,$d_{x2-y2}$) and $t_{2g}$ ($d_{xy}$, $d_{xz}$, $d_{yz}$).

For hexaaqua and catechol complexes, a LAVCP** basis set was used for heavy atoms and a 6-31g (tm) ** one for the other atoms. The ferric $[Fe(H_2O)_6]^{3+}$ and $[Fe(Cat)_2(H_2O)_2]^{-1}$ complexes were investigated under a sextet spin state while a quintet spin state was chosen for the ferrous analogs $[Fe(H_2O)_6]^{2+}$ and $[Fe(Cat)_2(H_2O)_2]^{-2}$ . These basis sets exhibit polarization and diffuse functions well adapted to inorganic ions and are implemented in the Jaguar program used in the present work[11].

### *2.2 Empirical force field*

The empirical SPASIBA (Spectroscopic Potential Algorithm for Simulating Biomolecular Conformational Adaptability) potential energy function includes classical and Urey-Bradley-Shimanouchi terms adapted to Infrared and Raman spectroscopic studies. It includes redundancies terms originating from tetrahedral constraints and additional trans-gauche terms. The particular form of this potential energy has been largely described elsewhere [12-14] and the related parameters (force constants) have been obtained for a large variety of chemical groups and biomolecular families (peptides, lipids, saccharides) from Raman and Infrared vibrational spectroscopies.

## 3. Results and Discussion

### *3.1. Fe(III) complexes $[Fe(H_2O)_6]^{3+}$ and $[Fe(Cat)_2(H_2O)_2]^{-1}$*

#### 3.1.1. DFT calculations

Table 1 displays the hybrid functionals, basis sets, and multiplicity states used in this work to describe the four complexes.

**Table 1.** Functionals and Basis sets used in DFT calculations.

| Complex | Method | Basis Set | Multiplicity | Global charge |
|---|---|---|---|---|
| $[Fe(H_2O)_6]^{3+}$ | B3LYP | 6-31G(tm)**+/LAVCP** | 6 (High Spin) | +3 |
| $[Fe(Cat)_2(H_2O)_2]^{-1}$ | B3LYP | LAVCP** | 6 (High Spin) | -1 |
| $[Fe(H_2O)_6]^{2+}$ | B3LYP | 6-31G(tm)**/6-31G(tm)**+ | 5 (High Spin) | +2 |
| $[Fe(Cat)_2(H_20)_2]^{-2}$ | B3LYP | LAVCP** | 5 (High Spin) | -2 |

The hexaaqua Fe(III)/($[Fe(H_2O)_6]^{3+}$ complexes displays an octahedral ferric/ferrous combination with six water molecules adopting a pratically pure $T_h$ molecular point group symmetry leading to a spherical symmetry (Figure 1) while the dipyrocatecholato Fe(III)/ ($[Fe(Cat)_2(H_2O)_2]^{-1}$ molecules derived from cathechol-iron complexes form an octahedral ferric/ferrous iron involving two catechol molecules and two water molecules [9] (Figure 2).

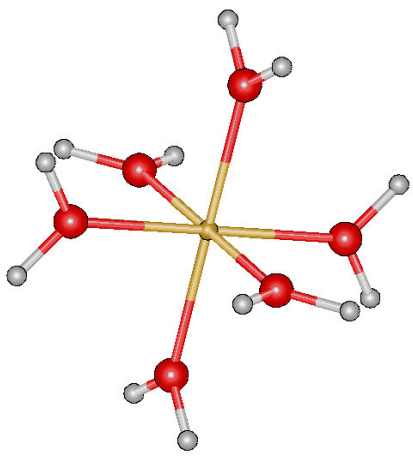

**Figure 1.** $[Fe(H_2O)_6]^{3+}$ ($T_h$ molecular point group)

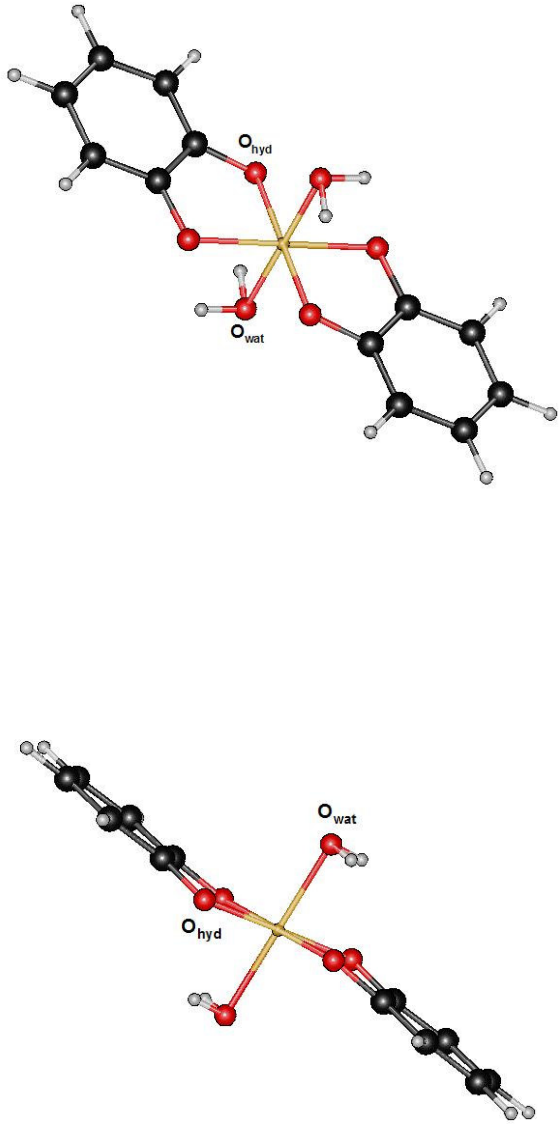


**Figure 2.** Schematic representation of the $[Fe^{(III/II)}(Cat)_2(H_2O)_2]$ complexes

Present DFT calculations on the hexaaqua Fe(III) complex structures lead to optimized geometrical values in a general agreement with previous quantum theoretical calculations carried out by Jarzecki et al. [8] on the hexaaqua complexes using the B3LYP method with different basis sets (Table 2a). In the present case, however, a longer Fe-O length of 2.052 Å was predicted when comparing with the 2.039 Å value obtained by Jarzecki et al. Values of 90° (direct angles) and 179°.95 are predicted for the O-Fe-O valence angles while for the Fe-O-H valence angles a mean value of 126°.4 could be obtained.

**Table 2a.** DFT (sextet electronic state) and SPASIBA optimized structural parameters for the ferric complex of $[Fe(H_2O)_6]^{3+}$.

| Parameters | Experimental | DFT | SPASIBA |
|---|---|---|---|
| Fe-O | 1.994-2.002[(a)] ,2.039[(b)] | 2.052(0.0) | 1.957-2.003(0.001) |
| O-H | 0.995-1.002[(a)],0.973[(b)] | 0.978(0.0) | 0.996(0.0) |
| O-Fe-O (direct angle) | 90.5-90.9[(a)] ,90.0[(b)] | 90.0(0.041) | 90.0(1.098) |
| O-Fe-O | - | 179.95(0.024) | 179.51(0.021) |
| Fe-O-H | - | 126.4(0.036) | 129.94(0.372) |
| H-O-H | 108.0-110.4[(b,c)] | 107.2(0.02) | 100.08(0.178) |

Bonds are given in Å and valence angles in degrees. Root Mean Square Deviations are given in parenthesis. Crystallographic data : (a) Cesium Sulphate $CsFe(SO_4)_2,12H_2O$ and (b) Selenate Alums $CsFe(SeO_4)_2,12H_2O$ (ref.[17]), (c) (ref[18]).

**Table 2b**. DFT (sextet electronic state) and SPASIBA optimized structural parameters for the ferric complex of $[Fe(Cat)_2(H_2O)_2]^{-1}$.

| Parameters | Experimental[(a)] | DFT | SPASIBA |
|---|---|---|---|
| $Fe-O_{wat}$ | 2.0 | 2.038 (0.105) | 1.957(0.029) |
| O-H | 0.96 | 0.95 (0.0) | 0.977 |
| C-C | 1.398 | 1.405 (0.011) | 1.404 |
| C-O | 1.364 | 1.340 (0.001) | 1.413 |
| C-H | 1.086 | 1.088 (0.0) | 1.100 |
| C-O-Fe | - | 109.51 (0.036) | 107.54 |
| C-C-C | 120.0 | 120.12 | 120.0 |
| C-C-O | 120.0 | 120.13 | 119.63 |
| O-Fe-O (direct angle) | 90.5-90.9 | 90.0 (0.041) | 90.0 |
| O-Fe-O | 180.0 | 179.97 (0.024) | 179.51 |
| Fe-O-C | - | 109.51 | 107.54 |
| Fe-O-H | - | 102.33 (0.014) | 110.0 |
| H-O-H | 104.5 | 104.2 (0.014) | 107.03 |
| Interplanar distance(in Å) | | 0.60 | 0.13 |

Bonds are given in Å and valence angles in degrees. Root Mean Square Deviations are given in parenthesis. The direct angles are defined by $O_{hyd}$-Fe-$O_{wat}$ angles with $O_{hyd}$ and $O_{wat}$ standing for hydroxyl and water oxygens respectively. [(a)] mean value (ref [19-20]) .C : Internal ring carbon atom.

The final optimized geometry of the Fe(III)-catechol complex $(Fe(Cat)_2(H_2O)_2]^{-1}$ displays a $C_{2h}$ molecular point group symmetry with the Fe atom located at the inversion center. As can be observed in Figure 2, the two ring planes adopt quasi parallel orientations displaying an mean interplanar distance of 0.6 Å and alternative angular values of 84.7° and 95.3° for the two direct $O_{hyd}$-Fe-$O_{wat}$ angles belonging to a same ring. By examination of Table 2b, one can observe a reasonable agreement

between the values of the optimized internal parameters and those extracted from X-Rays studies [15], ESR spectroscopy [16] or other experimental and calculated values reported by various auhors [17-20] . According to Funabiki et al. [19] a mean value of 2.Å for the Fe-O bond length must correspond to a minimum in the structural energy.

3.1.2. SPASIBA parameters for $Fe[(H_2O)_6]^{3+}$ -$[Fe(Cat)_2(H_2O)_2]^{-1}$

**Table 3**. Empirical SPASIBA force constants related to the $[Fe(H_2O)_6]^{3+}$ and $[Fe(Cat)_2(H_2O)_2]^{-1}$ /Fe(III) complexes.

| Bonds | K (Kcal.mol$^{-1}$) | $R_0$ (Å) | |
|---|---|---|---|
| Fe-$O_{hyd}$ | 117.0 | 2.00 | |
| Fe-$O_{wat}$ | 117.0 | 2.00 | |
| O-H | 511.0 | 0.98 | |
| C-O | 315. | 1.41 | |
| C-C | 2.90 | 1.40 | |
| Valence angle | H (Kcal.mol$^{-1}$.rad$^{-2}$) | $\Theta_0$ (degrees) | F(Kcal.mol$^{-1}$. Å$^2$) |
| $O_{hyd}$-Fe-$O_{hyd}$* | 10.0 | 91.0 | 9.0 |
| $O_{hyd}$-Fe-$O_{hyd}$** | 10.0 | 91.0 | 9.0 |
| $O_{hyd}$-Fe-$O_{hyd}$** | 10.0 | 179.0 | 9.0 |
| $O_{hyd}$-Fe-$O_{wat}$ | 10.0 | 91.0 | 9.0 |
| C-O-Fe | 41.0 | 109.0 | 19.0 |
| Fe-O-H | 20.0 | 120.0 | 0. |
| H-O-H | 33.0 | 107.0 | 91.0 |
| C-C-O | 34.0 | 120.0 | 85.0 |
| C-C-H | 32.0 | 120.0 | 0. |
| C-C-C | 45.0 | 120.0 | 30. |
| C-O-Fe | 41.0 | 109.0 | 19. |
| Torsions | Vn/2(Kcal.mol$^{-1}$) | Phase (degrees) | n (order) |
| X-Fe-O-X | 0.045 | 0.0 | 3 |

C : (ring carbon atom),, H:(hydrogen on C), hyd : hydroxyl, wat : water *Hydroxyl groups belonging : * to the same ring and ** to different rings.

The SPASIBA parameters (Table 3) associated to the two Fe(III) complexes were obtained from normal coordinate analyses using experimental and DFT vibrational frequencies partly obtained from the work of Jarzecki et al.[8].

The present DFT vibrational frequencies and the associated potential energy distribution (P.E.D) among internal coordinates were derived via the Redong program (Allouche and Pourcin [21]) using a general scaling factor of 0.962 applied to each internal force constants to fit the theoretical and the experimental data. Such a factor is generally used to give correct agreements with experiments[22].

For the $[Fe(H_2O)_6]^{3+}$ complex (Table 2a), the Fe-O bond length value obtained after geometry optimization is in accordance with the experimental values(1.99-2.002Å)and the root mean square deviation confirms the presence of equivalent bonds enforcing the $d^5$ electronic structure of $Fe^{3+}$. The related values associated to O-H bond lengths and the Fe-O-H valence angle values correspond to the predicted DFT results.

The SPASIBA optimized value associated to the H-O-H valence angle (100.8°) displays however a relative large discrepancy when compared to the DFT and experimental data (107-108.°). The reason for this is not clear but the general $T_h$ symmetry is not pertubated. The same set of SPASIBA force constants associated to the Fe-O, O-Fe-O, H-O-H, Fe-O-H internal coordinates was presently used along the normal mode analyses of the $[Fe(Cat)_{2(}H_2O)_2]^{-1}$ complex (Table 3).

Since no exprimental vibrational data are available, comparizons were directly done with the DFT derived vibrational frequencies in one hand, and, in a second hand, with the characteristic values observed for the various chemical groups [18-20]. The empirical values associated with the internal coordinates of the catechol complex after minimization are reported in Table 2b and display a general good agreement with the experimental and predicted DFT values with a very weak distance of 0.13-0.20 Å between the two catechol molecular planes .

The optimized Fe-Owater derived bond lengths (1.957Å/empirical) and (2.038Å/DFT) are close to the experimental value (~2Å)while the empirically optimized Fe-O-H valence angle value is higher (110.0°) than the corresponding DFT predicted one(102.33°). Both calculations give comparable values for the Fe-C-O valence angle i.e. 107.4° (SPASIBA) and 109.51° (DFT). The carbon-oxygen bond lengths however display also important differences (-0.02Å for DFT and +0.05Å for the empirical SPASIBA force field when compared to the experimental value(1.364Å).

Using the same set of empirical force constants in the two ferric complexes $[Fe(H2O)_6]^{3+}$ and $[Fe(Cat)_2(H_2O)_2]^{-1}$ ,one can note similarities for the Fe-O, O-H bonds and O-Fe-O, H-OH valence angles excluding however the Fe-O-H angle as discussed before. One explanation would stand in different vibrational motions of the water molecules bound to iron for the two complexes.

### 3.1.3. Normal modes analysis

Rotational motions related to the Fe-O bond are predicted to occur at low wavenumbers in similar ranges (32-275 $cm^{-1}$ for SPASIBA) and (59-259 $cm^{-1}$ for DFT) . Empirical derived vibrational frequencies related to the O-Fe-O bending in plane motions spread over the 247-330 $cm^{-1}$ range in agrement with the DFT predicted values (275-357 $cm^{-1}$) . A same general accordance exists for the Fe-O-C and Fe-O-H in plane bending motions and for the Fe-O stretching mode (Table 4).

**Table 4.** Experimental and calculated vibrational wavenumbers (in $cm^{-1}$) for the $[Fe(H_2O)_6]^{3+}$ and $[Fe(Cat)_2(H_2O)_2]^{-1}$ ferric complexes.

| Assignments | Exp.[(a)] | DFT | SPASIBA |
|---|---|---|---|
| τ Fe-O | | 59.1-258.8 | 32.9-274.7 |
| δ O-Fe-O | 306-332 | 275.6-357.3 | 247.7-330.1 |
| ν Fe-O | 475-523 | 349.8-493 | 371-495.6 |
| δ Fe-O-C | - | 746.1-774.8 | 736.2-736.7 |
| | | 404.7-517.4[(1)] | 433.7-511.4[(1)] |
| δ Fe-O-H | 721-746[(2)] | 641.5-646.1[(2)] | 672-690.6[(2)] |
| | | 867.8-914.2[(3)] | 889.7-937.7[(3)] |

τ : torsion, ν : stretching, δ : in plane bending. [(a)] Raman spectra of $CsFe(SO_4)_2.12H_2O$ and $CsFe(SeO_4).12H_2O$ [8,23].
(1) out and (2) in plane bending of the $Fe(H_2O)$ plane in $[Fe(H_2O)_6]^{3+}$ (3): $[Fe(Cat)_2(H_2O)_2]^{-1}$

The vibrational assigments provided by the empirical normal mode treatments seem acceptable when compared to available experimental values extracted from Cesium sulphate $CsFe(SO_4)_2.12H_2O$ and Selenate alums $CsFe(SeO_4)_2.12H_2O$ [8,17] particularly for the O-Fe-O bending and Fe-O stretching modes. The 672-691 $cm^{-1}$ wavenumber range obtained from empirical normal mode analysis related to in plane bending modes Fe-O-H occuring in the $Fe[(H_2O)_6]^{3+}$ complex can be easily related to experiments (721-746$cm^{-1}$). The discreapencies in vibrational wavenumbers observed for the Fe-O bonds between empirical or DFT vibrational frequencies and experiments could be explained by crystallin effects.

### *3.2. $[Fe(H_2O)_6]^{2+}$ -$[Fe(Cat)_2(H_2O)_2]^{-2}$ Fe(II)complexes*

#### 3.2.1. DFT calculations

In the $[Fe(H_2O)_6]^{2+}$ complex, the $Fe^{2+}$ ion displays a $d^6$ electronic configuration and forms an octahedral complex subject to Jahn-Teller distorsions constraining the molecular point group to adopt a $C_i$ symmetry to form a stable conformation [8]. Table 5 displays the optimized DFT and minimized SPASIBA internal coordinates obtained for the two complexes.

In the ferrous complexes, the Fe-O bond length increases by about 0.05Å when regarding to the corresponding experimental DFT and empirical values obtained for the $Fe^{3+}$ hexaaqua complex and, to a less extent, by a smaller value (0.03Å) for the catechol ferric complex. The Fe-O-H valence angles display similar values for both the ferric and ferrous hexaaqua (124-129°) complexes while the corresponding values obtained from DFT and empirical calculations adopt smaller values for the catechol complexes (102-110°) .

**Table 5a**. Structural parameters obtained from DFT geometry optimization and empirical minimization performed onto the $[Fe(H_2O)_6]^{2+}$ complex.

| Parameters | Exp. (a) | DFT | SPASIBA |
|---|---|---|---|
| Fe-O | 2.098-2.143 | 2.085-2.143 | 2.02-2.077 |
| O-Fe-O | 89.25-91.02 | 90.0 | 89.96-90.0 |
| O-Fe-O | - | 179.79 | 179.35 |
| Fe-O-H | - | 124.81 | 127.92 |
| H-O-H | | 110.38 | 103.93 |

Bond lengths are given in Å and valence angles in degrees. (a)Experimental values extracted from ammonium salts $(NH_4)_2[Fe(H_2O)_6](SO_4]_2$ (ref.8,24)

**Table 5b**. Mean structural parameters values obtained from DFT geometry optimization and empirical minimization on the $[Fe(Cat)_2(H_2O)_2]^{-2}$ complex.

| Parameters | Exp. (b) | DFT | SPASIBA |
|---|---|---|---|
| Fe-O | 2.06-2.19 | 2.085 | 2.02 |
| O-H | 0.96 | 0.98 | 0.981 |
| C-C | 1.398 | 1.411 | 1.406 |
| C-O | 1.364 | 1.327 | 1.337 |
| C-H | 1.086 | 1.091 | 1.089 |
| C-O-Fe | 120.0 | 111.97 | 110.52 |
| C-C-C | 120.0 | 120.0 | 120.0 |
| C-C-H | 120.0 | 119.69 | 120.1 |
| C-C-O | 120.0 | 120.61 | 119.69 |
| O-Fe-O | 90.0 | 90.0 | 90.0 |
| O-Fe-O | 180.0 | 180.0 | 179.37 |
| Fe-O-H | - | 106.6 | 107.69 |
| H-O-H | 104.5 | 100.15 | 105.02 |
| Interplanar distance (Å) | | 0.49 | 0.20 |

Bond lengths are given in Å and valence angles in degrees. C : ring carbon atoms. (b) Experimental values extracted from ref [8,18,19,24,26-33].

The DFT optimized geometry related to the$[Fe(Cat)_2(H_2O)_2)]^{-2}$ complex displays a similar $C2_h$ molecular point group symmetry with an interplanar distance of about 0.5 angströms between the two catechol molecular planes with $O_{hyd}$-Fe-$O_{wat}$ valence angles (belonging to a same ring) adopting values of 72.5° and 107.5°.

3.2.2. SPASIBA parameters for the Ferrous complexes

After vibrational normal modes analyses and vibrational frequencies refinements on the ferrous complexes, the final derived empirical Fe-O stretching force constant appears as being the most affected with an associated force constant decreasing from K=117.0 ($Fe^{3+}$) to 65.0 ($Fe^{2+}$) $kcalmol^{-1}Å^{-2}$ while in plane valence angle bending and torsional parameters remain essentially unchanged (Table 6).

**Table 6.** Final force constants deduced from SPASIBA empirical calculations carried on the Ferrous $[Fe(H_20)_6]^{2+}$ and $[Fe(Cat)_2(H2O)_2]^{-2}$ complexes.

| Bonds | K(kcal.mol$^{-1}$Å) | Ro(Å) | |
|---|---|---|---|
| Fe-O | 65.0 | 2.13 | |
| O-H | 511.0 | 0.98 | |
| C-O | 315.0 | 1.41 | |
| C-C | 290. | 1.40 | |
| Bendings | H(kcal.mol$^{-1}$.rad$^{-2}$) | $\theta_o$(degrees) | F(kcal.mol$^{-1}$.Å$^{-2}$) |
| O-Fe-O | 4.0 | 89.0 | 2.0 |
| O-Fe-O | 4.0 | 179.0 | 2.0 |
| C-O-Fe | 46.0 | 112.0 | 21.0 |
| Fe-O-H | 18.0 | 120.0 | 0.0 |
| C-C-O | 34.0 | 120.0 | 85.0 |
| C-C-H | 32.0 | 120.0 | 0. |
| C-C-C | 45.0 | 120.0 | 30. |
| C-O-Fe | 46.0 | 112.0 | 21.0 |
| Torsions | Vn/2(kcalmol$^{-1}$) | Phase(degrees) | n (order) |
| X-Fe-O-X | 0.043 | 0.0 | 3. |
| X-CA-CA-X | 3.925 | 180.0 | 2. |
| X-CA-O-X | 1.80 | 180.0 | 2. |

C : ring carbon atom

3.2.3. Normal modes

The Fe-O torsional modes are predicted in the 30-130 $cm^{-1}$ range in agreement with the corresponding values obtained for the Fe(III) complexes (Table 7). Experimental bands corresponding to the in plane bending δ(O-Fe-O) normal mode observed in the 210-231 $cm^{-1}$ range are predicted to occur in the 80-230 $cm^{-1}$ range by both DFT and empirical methods. This wavenumber range seems characteristic of the Fe(II) type complexes when compared to the Fe(III) complexes in which predicted values stand in the 350-500 $cm^{-1}$ range with experimental bands observed between 475 and 532 $cm^{-1}$. In a similar way, the stretching ν(Fe(II)-O) motion is predicted to participate to normal modes at lower wavenumbers (exp .296-380, DFT/SPASIBA. 240-515 $cm^{-1}$) than when dealing with Fe(III) complexes (exp.475-523,DFT/SPASIBA. 350-496 $cm^{-1}$). For both the Fe(III)/Fe(II) complexes and according to the fact that iron is bound or not to catechol molecules, the δFe-O-H bending motion is predicted to

participate to normal modes along different vibrational wavenumbers range i.e. 520-690 $cm^{-1}$ for the hexaaqua complexes and 850-940 $cm^{-1}$ in the catechol complexes.

**Table 7**. Calculated and observed vibrational wavenumbers (in $cm^{-1}$) of the two ferrous complexes $[Fe(H_2O)_6]^{2+}$ and $[Fe(Cat)_2(H_2O)_2]^{-2}$.

| | Exp. (a) | DFT | SPASIBA |
|---|---|---|---|
| τ Fe-O | - | 33-117.3 | 39.2-137.5 |
| δ O-Fe-O | 210-231 | 81.3-258.7 | 97.3-228.8 |
| ν Fe-O | 296-379 | 242.1-515.9 | 269 –493.7 |
| δ Fe-O-C | - | 712.7-714.2 | 725.4-726.5 |
| δ Fe-O-H | - | 524.4-688(1) | 509.1-674.5(1) |
| | | 857.6-882.5(2) | 871.3-906.3(2) |

ν : stretching, δ : in plane bending, τ : torsion (a) Raman bands from hexafluorosilicate salts $FeSi.6H_2O$[ ref.25]
(1) $[Fe(H_2O)_6]^{2+}$ ,(2) $[Fe(Cat)_2(H_2O)_2]^{-2}$

3.2.4. Normal modes related to the catechol part in FeIII/FeII complexes

A general set of empirical force constants related to the phenolic part was used for both complexes and a general root mean square deviations of 19 $cm^{-1}$ was obtained when comparing SPASIBA to DFT derived wavenumbers. A reasonably good accordance could be obtained in the present work with the few available experimental data [28,30,33,34].

The predicted SPASIBA vibrational wavenumbers related to torsional C-C motions between ring carbon atoms (C) present contributions at (195,256,262,308, 351,450,579-636,690-697,736-739, 828-832) $cm^{-1}$ and have to be compared with DFT values (188,215,237,327,339,484-602,701-712,727-735,843-853) $cm^{-1}$. Corresponding experimental wavenumbers are observed at 244,503,686, 751,823 and 881 $cm^{-1}$).

Torsional C-O motions are generally coupled with C-C torsional contributions and have been calculated at 261.7(SPASIBA), 237.6(DFT) $cm^{-1}$ in the present woork. These values can be correlated to the experimental value (309$cm^{-1}$).

The δC-C-C bending modes predicted to occur at 537,637,884 $cm^{-1}$(SPASIBA), 527, 605 and 875 $cm^{-1}$(DFT) are in agrement with experimental values observed at 527, 619, 817 and 958 $cm^{-1}$. The experimental 296 $cm^{-1}$ band associated to the δC-C-O valence angle bending is satisfactorily reproduced by DFT/SPASIBA calculations (242/269 $cm^{-1}$). Other angular motions such as δC-C-H display calculated contributions in the following ranges i.e. 1271-1304/1460-1596 $cm^{-1}$ (SPASIBA) and 1293-1322/ 1470-1602 $cm^{-1}$ (DFT) and have to be compared with corresponding experimental values (1272,1343,1472,1501 $cm^{-1}$).

The stretching CA-CA motions have predicted wavenumbers spreading over 756-799, 1034-1149 $cm^{-1}$ (SPASIBA) and 785-826,1018-1152 $cm^{-1}$ (DFT). Such vibrations are largely coupled with δC-C-H motions in the 1271-1374,1530-1596 $cm^{-1}$ range (SPASIBA) and over 1293-1367,1534-1602 $cm^{-1}$ (DFT). Available related experimental values can be observed at 751,817,1072,1151,1603 and 1610 $cm^{-1}$.

Other stretching modes such as C-O have vibrational wavenumbers in the 1149-1284 (SPASIBA) and 1151-1309 (DFT) $cm^{-1}$ ranges. These two regions include the characteristic experimental band assigned to this mode observed at 1275 $cm^{-1}$.

High frequency vibrational ranges related to C-H symmetric and antisymmetric stretching motions (3114-3121 /SPASIBA and 3099-3160 $cm^{-1}$/DFT) can be fitted with the 3027,3049 and 3070-3075 $cm^{-1}$) observed ones. O-H stretching modes have comparable predicted DFT/SPASIBA wavenumbers in the 3647-3766 $cm^{-1}$) range. Both DFT and the SPASIBA empirical force field under use reproduce satifactorily the mean vibrational features related to the phenolic groups.

## Conclusion

A preliminary determination of the empirical SPASIBA force field devoted to aqueous and cathecolate complexes with Fe(III) and Fe(II) was carried out. Geometrical parameters and vibrational frequencies obtained from normal mode analyses on hexaaqua and dicatechol-water ($Fe^{3+}/Fe^{2+}$) complexes have been compared to experimental and theoretical quantum DFT values . The same set of force constants could be used for both FeIII/FeII complexes apart for that related to the Fe-O stretching which has to be chosen according to the electronic state of spin under consideration A generally good agreement between all methods was observed. Further calculations are in progress to apply this force field for Molecular Dynamics which would permit to follow the complex formation and its evolution along physicochemical constraints (pH, temperature, counter-ions or external competitive ligands) keeping in mind the biochemical importance of iron releasing in organisms.

## References

1. Spencer, C. M.; Cai, Y.; Martin, R.; Gaffney, S. H.; Goulding, P. N.; Magnolato, D.; Lilley, T. H.; Haslam, E. Polyphenol complexation –Some thoughts and observations. *Phytochemistry* **1988**, *27*, 2397-2409.
2. Horton, S.; Levin, C. Commentaries on "Evidence that Iron deficiency Anemia causes reduced work capacity". *J. Nutr*. **2001**, *131*, 691S-696S.
3. Cook, J. D.; Reddy, M. B.; Hurrel, R. F. The effect of read and white wines on nonheme-iron absorption in Humans. *Am. J. Clin .Nutr.* **1995**, *61*, 800-804.
4. Frankel, E. N.; German, J. B.; Kinsella, J. E.; Parks, E.; Kanner, J. Inhibition of oxidation of human low-density lipoprotein by phenolic substance in red wine. *The Lancet* **1993**, *341*, 454-457.
5. Lokman, K.; Haslam, E.; Williamson, M. P. Structure and conformation of the procyanidin $B_2$-dimer. *Magnetic Resonance in Chemistry* **1997**, *35*, 854-858.
6. Hemingway, R. W.; Tobiason, F. L.; Wayne Mc Graw, G.; Steynberg, J. P. Conformation and complexation of tannins: NMR spectra and Molecular Search Modeling of Flavan-3-cis Magnetic Resonance in chemistry. *Magnetic Resonance in Chemistry* **1996,** *34*, 424-433.
7. Lambrinidis, G.; Halabalaki, M.; Katsanou, E. S.; Skaltsounis,A. L.; Alexis, M. N.; Mikros, E. The estrogen receptor and polyphenols: molecular simulation studies of their interactions, a review. *Environnmental Chemistry Letters* **2006**, *4*, 159-174.
8. Jarzecki, A. A.; Anbar, A. D.; Spiro, T. G. DFT Analysis of $Fe(H20)_6^{3+}$ and $Fe(H20)_6^{2+}$. Structure and vibrations; Implications for Isotope Fractionation. *J. Phys. Chem. A* **2004**, *108*, 2726-2732.

9. Yamahara, R.; Ogo, S.; Masuda, H., Watanabe, Y. J. (Catecholato) iron(III) complexes: Structural and functional models for the catechol-bound iron(III) form of catechol dioxygenases. *Inorg. Biochem.* **2002**, *88*, 284-294.
10. Wong, M. W. Vibrational frequency prediction using density functional theory. *Chem. Phys. Letters* **1996**, *256*, 391-399.
11. Jaguar Program, v.4.0 ; Schrödinger, Inc. : Portland, OR, 1999.
12. Derreumaux, P.; Vergoten, G. A new spectroscopic molecular mechanics force field. Parameters for proteins. *J. Chem. Phys.* **1995**, *102*, 8586-8605.
13. Vergoten, G.; Mazur, I.; Lagant, P.; Michalski, J. C.; Zanetta, J. P. The SPASIBA force field as an essential tool for studying the structure and dynamics of saccharides. *Biochimie* **2003**, *85*, 65-73.
14. Lagant, P.; Nolde, D.; Stote, R.; Vergoten, G.; Karplus, M. Increasing normal mode analysis accuracy: The SPASIBA spectroscopic force field introduced into the CHARMM Program. *J. Phys. Chem. A.* **2004**, *108*, 4019-4029.
15. Orville, A. M.; Lipscomb, J. D.; Ohlendorf, D. H. Binding of isotopically labeled substrates inhibitors, and cyanide by protocatechuate 3,4-dioxygenase. *J. Biol. Chem.* **1989**, *264*, 8791-8801.
16. Whittaker, J. W.; Lipscomb, J. D.; Kent, T. A.; Münck. E. Brevibacterium fuscum protocatechuate 3,4-dioxygenase. Purification, crystallization and characterization. *J. Biol. Chem.* **1984**, *259*, 4466-4475.
17. Best, S. P.; Forsyth, J. B. Stereochemistry of tervalent aqua ions: Low-temperature Neutron Diffraction. Structure of $CsFe(SO_4)_2.12H_2O$ and $CsFe(SeO_4)_2.12H_2O$ *J. Chem. Soc. Dalton Trans.* **1990**, 395-400.
18. Durier, V.; Tristram, F.; Vergoten, G. Molecular force field development for saccharides using the SPASIBA spectroscopic potential. Force field parameters for α-D-Glucose. *J. Mol. Struct. (Theochem)* **1997**, *395-396*, 81-90.
19. Funabiki, T.; Yamazaki, T. Mechanism of oxygenative cleavage of catechols by nonheme iron complexs in relevance to catechol dioxygenases studied by quantum chemical calculations. *Journal of Molecular Catalysis. A: Chemical* **1999**, *150*, 37-47.
20. Torrens, F. Nature of $Fe^{III}$-O2, $Fe^{II}$-CO and $Fe^{III}$-CN complexes of hemoprotein models. *Polyhedron* **2003**, *22*, 1091-1098.
21. Allouche, A.; Pourcin,B. Ab initio calculation of vibrational force fields: Determination of non-redundant symmetry coordinates by least-square component analysis. *Spectrochim. Acta* **1993**, *49A*, 571-580.
22. Pulay, P. Possibilities and limitations of ab initio calculatio of vibrational spectra. *J.Mol.Struct.* **1995**, *347*, 293-308.
23. Best, S. P.; Armstrong, R. S.; Beattie, J. K.; Single-crystal Raman spectroscopy of the α-Alums $CsM(SO_4)_2.12H_2O$ (M=Co or Ir) between 275 and 1200 $cm^{-1}$). *J. Chem. Soc., Dalton Trans.* **1992**, 299-304.
24. Cotton, F. A; Daniels, L. M.; Murillo, C. A.; Quesada, J. F. Hexaaqua dispositive ions of the first transition series: new and accurate structures; expected and unexpected trends. *Inorg. Chem.* **1993**, *32*, 486.

25. Jenkins, T. E.; Lewis, J. A Raman investigation of some metal(II) hexafluorosilicate(IV) and hexafluorotitanate(IV) salts. *Spectrochim. Acta. PartA: Mol. Spectrosc.* **1981**, *37A*, 47-50.
26. Merlel, M.; Muller, V.; Krebs, B. Novel iron(III) comolexes with phenolate containing tetradentate ligands as model systems for catechol 1,2-dioxygenase. *Inorganica Chimica Acta* **2002**, *337*, 308-316.
27. Joseph, M.; Suni, V.; Nayar, C. R.; Kurup, M. R. P.; Hoong-Kun-Fun. Synthesis, spectral characterization and crystal structure of 2-benzylpyridine N(4) cyclohexylthiosemicarbazone. *J. Mol. Struct.* **2004**, *705*, 63-70.
28. Chis, V. Molecular and vibrational structure of 2,4 dinitrophenol: FT-IR, FT-Raman and quantum chemical calculations. *Chem. Phys.* **2004**, *300*, 1-11.
29. Kagawa, T.; Kawai, R.; Kashino, S.; Haisa, M. The crystal and molecular structure of 2,4 dinitrophenol. *Acta. Cryst. B32* **1976**, 3171.
30. Cabral, B. J. C.; Gil, R.; Fonseca, B.; Simoes, J. A. M. Density functional and density functional reaction field calculations of the molecular properties of phenol. *Chem. Phys. Lett.* **1996**, 258, 436-444.
31. Hämäläinen, R.; Urpeinen, U. The structure, Thermal and Magnetic properties of hexaquaion(II) bis[bis(N-salicylideneglycinato) ferrata(III)] dihydrate. *Acta. Chem. Scand.* **1989**, *43*, 15-18.
32. Scott, R.; Wang, S.; Eidsness, M. K.; Kriauciunas, A.; Frolich, C. A.; Chen, V. J. X-ray absorption spectroscopic studies of the high-spin iron(II) active site of isopenicillin N-synthase: evidence for iron-sulfur interaction in the enzyme-substrate complex. *Biochemistry* **1992,** *31*, 4596-4601.
33. Dimitrimova, Y. Ab initio and DFT studies of the vibrational spectra of hydrogen-bonded phOH $(H_2O)_4$ complexes. *Spectochim. Acta, Part A.* **2004**, *60*, 3049-3057.
34. Sanchez-Cortès, S.; Garcia-Ramos, J. V. Adsorption and chemical modification of phenols on a silver surface. *Journal of Colloid and Interface Science* **2000**, *231*, 98-106.

© 2007 by MDPI (http://www.mdpi.org). Reproduction is permitted for noncommercial purposes.